Stony Brook University

Functional consequences of a putative Mek1 phosphorylation site on Rad17 during meiosis in *Saccharomyces cerevisiae*

A Thesis Presented

by

Madeeha Rahat

to

The Graduate School

in Partial Fulfillment of the

Requirements

for the Degree of

Master of Science

in

Biochemistry and Cell Biology

Stony Brook University

December 2016

Stony Brook University
The Graduate School

Madeeha Rahat

We, the thesis committee for the above candidate for the

Master of Science degree, hereby recommend

acceptance of this thesis.

Nancy M. Hollingsworth
Professor, Department of Biochemistry and Cell Biology

Aaron Neiman
Professor and Chair, Department of Biochemistry and Cell Biology

This thesis is accepted by the Graduate School

Charles Taber
Dean of the Graduate School

Abstract

Functional consequences of a putative Mek1 phosphorylation site on Rad17 during meiosis in *Saccharomyces cerevisiae*

by

Madeeha Rahat

Master of Science

in

Biochemistry and Cell Biology

Stony Brook University

December 2016

Meiosis is a specialized type of cell division, which produces haploid daughter cells from diploid parental cells. Meiotic recombination is initiated by the introduction of programmed DNA double strand breaks (DSBs), which are catalyzed by an evolutionarily conserved, meiosis-specific endonuclease, Spo11. Meiotic cells monitor the repair of Spo11-induced DSBs via the meiotic recombination checkpoint (MRC), which is activated in response to DSBs made during meiotic prophase. The MRC ensures proper repair of DSBs prior to entry into the first meiotic division. The Mec1 checkpoint kinase is recruited to resected DSBs via the 9-1-1 complex containing Rad17, Mec3 and Ddc1. Mec1 phosphorylation of Hop1 allows recruitment of the meiosis-specific kinase Mek1 to chromosomes where Mek1 is activated. Mek1 phosphorylation of substrates then ensures that DSBs are repaired in a Dmc1-dependent manner. My thesis focused on identifying the consequences of a putative Mek1 phosphorylation site on Rad17 in an attempt to further understand the function of Mek1 in meiosis in the budding yeast, *Saccharomyces cerevisiae*.

Table of Contents

Figures and Tables

List of Abbreviations

A	alanine
Amp	Ampicillin
bp	base pairs
BSA	Bovine Serum Albumin
C	cytosine
CO	crossover
D	aspartic Acid
DNA	deoxyribose nucleic acid
D-loop	displacement loop
dHJ	double Holliday Junction
DMSO	dimethyl sulfoxide
dNTPs	deoxynucleotide triphosphates
DSB	double strand breaks
EDTA	Ethylenediaminetetraacetic acid
EtOH	Ethanol
G	guanine
H_2O	water
K	lysine
Kan	Kanamycin
kb	kilo base
L/H	light/heavy

LB	Lysogeny broth
mL	milliliter.
MRC	meiotic recombination checkpoint
N	primer length in bases
NAT	Nourseothricin
NCO	noncrossover
NEB	New England Biolab
ng	Nano gram
PCNA	proliferating cell nuclear antigen
PCR	polymerase chain reaction
ORF	open reading frame
PEG	Polyethylene glycol
R	arginine
rpm	revolutions per minute
SD	synthetic defined
SDS	sodium dodecyl sulfate
SDSA	synthesis dependent strand annealing
SILAC	stable Isotope Labeling by Amino acids in Cells
ssDNA	single strand DNA
T	threonine
T_m	melting temperature
TAE	Tris-acetate Ethylenediaminetetraacetic
TBE	Tris-borate ethylenediaminetetraacetic acid

TE	Tris- ethylenediaminetetraacetic acid
μL	microliter
UV	ultraviolet
V	volt
YPD	yeast extract peptone dextrose medium
ZMM proteins	Zip1, Zip2, Zip3, Zip4, Mer3, Msh4, Msh5, Spo16

Acknowledgements

I would like to thank my advisor Dr. Nancy Hollingsworth for allowing me to work in her lab. Her patience, constant feedback and infinite guidance has allowed me to learn a great deal from her. I would like to thank Dr. Neta Dean and the M.S Biochemistry and Cell Biology program at Stony Brook University. I would also like to thank Dr. Aaron Neiman, for serving as my supplemental reader. A very special thanks to Dr. Xiangyu Chen for helping me learn all the techniques that were essential to carry out this project. I would also like to thank the other members of the Hollingworth lab: Lihong Wan, Cameron Burnett and Evelyn Prugar.

I would like to take this opportunity to extend my sincerest gratitude to my parents and friends for their constant motivation and support during this journey.

Introduction

Meiosis: a specialized cell division required for sexual reproduction

Meiosis is derived from a Greek word meaning reduction (Farmer and Moore, 1905). Meiosis is a specialized type of cell division, which involves production of haploid daughter cells from diploid parental cells. The halving of the number of chromosomes is achieved by the cells going through one round of DNA replication, followed by two rounds of chromosome segregation. Homologous chromosomes segregate to opposite poles during Meiosis I and sister chromatids segregate during Meiosis II. This type of cell division is necessary for the production of gametes, which are essential for sexual reproduction. Meiosis ensures that the number of chromosomes remains constant from one generation to another. The fusion of two haploid gametes during sexual reproduction reinstates the ploidy of the new individual [Petronczki et al., 2003].

In eukaryotic cells, the sister chromatids created by DNA replication remain attached to one another via cohesion until the onset of anaphase [Nasmyth et al., 2000]. During meiotic prophase homologous chromosomes interact with each other through recombination, generating at least one crossover per chromosome. Crossovers, in combination with sister chromatid cohesion, create physical connections between homologs, allowing them to orient properly at Metaphase I, thereby ensuring accurate segregation [Buonomo et al., 2000; Henry et al., 2006] (Figure 1). Improper segregation of homologs during Meiosis I can lead to aneuploidy; a condition in which the number of chromosomes in daughter cells is not an exact multiple of the haploid number; for example Down syndrome is caused by an extra copy (triplicate) of chromosome 21 [Hassold and Hunt, 2001].

Meiotic recombination

Meiotic recombination between homologous chromosomes is highly regulated to ensure that every pair of homologs receives at least one crossover. Meiotic recombination is initiated by the introduction of programmed DNA double strand breaks (DSBs), which are catalyzed by an evolutionarily conserved, meiosis-specific endonuclease, Spo11, and other accessory factors [Keeney et al., 1997] (Figure 2). DSBs are perilous to the genome because if not repaired properly, pieces are lost when cells try to segregate broken chromosomes and the gametes are unable to produce viable progeny. DSBs are distributed non-randomly through out the genome in distinct regions known as hotspots [Keeney et al., 1997].

The 5' ends of the DSBs are removed in a process known as resection to generate 3' single strand ends (Figure 2). The mitotic recombinase, Rad51, and the meiosis specific recombinase, Dmc1, bind the single stranded DNA ends of the breaks to form nucleoprotein filaments [Brown et al., 2015]. These filaments search for homology on an intact homologous double strand of DNA, which serves as a repair template, thus mediating reciprocal exchange (i.e., crossovers) between homologous chromosomes [Brown et al., 2015]. A meiosis-specific kinase called Mek1 plays a role in ensuring that strand invasion occurs preferentially into the non-sister chromatid of the homolog [Wan et al., 2004; Kim et al., 2010]. Mek1 is the master regulator of meiotic recombination in budding yeast [Hollingsworth, 2016].

Dmc1, with the help of Rad51 and other proteins such as Hed1, functions to promote interhomolog crossovers (COs) [Bishop, 1994; Tsubouchi H. and Roeder GS. 2006]. Noncrossovers (NCOs) are created predominantly by DSB repair using synthesis-

dependent strand annealing (SDSA) [Allers and Lichten, 2001]. COs are promoted in meiosis using the ZMM pathway, which uses a group of proteins known as the ZMM proteins (Zip1-4, Mer3, Msh4, Msh5, Spo16), that stabilizes interhomolog strand invasion intermediates to create double Holliday junctions (dHJs) that are resolved only into COs [Börner et al., 2004; Allers and Lichten, 2001]. A minor number of dHJs are formed in the absence of the ZMM pathway. These dHJs are resolved in an unbiased way to give both COs and NCOs [De Muyt et al., 2012].

The meiotic recombination checkpoint

Meiotic cells monitor the repair of Spo11-induced DSBs via the meiotic recombination checkpoint (MRC) [Lydall et al., 1996; Subramanian and Hochwagen, 2014]. The MRC is activated in response to DSBs made during meiotic prophase and is a complex pathway that ensures proper repair of DSBs prior to entry into the first meiotic division [Subramanian and Hochwagen, 2014]. These checkpoints are conserved from budding yeast to humans. In budding yeast Tel1 and Mec1, orthologs of human protein serine/threonine kinases ATM and ATR respectively, are the master regulators of the checkpoint response [Gobbini et al., 2013].

In mitotically dividing budding yeast cells, DSBs activate Mec1/Tel1, which phosphorylate an adaptor protein called Rad9, which results in the recruitment of an FHA-domain containing effector kinase Rad53, resulting in a G2 delay to provide time for DSB repair to occur [Gobbini et al., 2013; Subramanian and Hochwagen, 2014; MacQueen and Hockwagen, 2011]. In addition to Rad53, other radiation repair genes or Rad genes play a vital role in the repair of the meiotic DSBs. In budding yeast, the 9-1-1 complex composed of Ddc1, Mec3 and Rad17, is a related to the replication protein known as proliferating cell

nuclear antigen (PCNA), and plays key roles in checkpoint activation and DNA repair [Parrilla-Castellar et al., 2004]. Mec1, a conserved checkpoint sensor kinase, detects ssDNA, recruits the 9-1-1 complex to the double strand/single strand junctions of the resected ends, where it is loaded around the DNA by Rad24-containing clamp loader [Parrilla-Castellar et al., 2004]. The 9-1-1 complex facilitates recruitment of checkpoint and repair proteins, allowing ATR-mediated phosphorylation and activation of Chk1 effector kinases. Chk1 regulates S-phase progression, G2/M arrest and replication fork stabilization [Parrilla-Castellar et al., 2004; Sancar et al., 2004].

In meiotic cells the MRC is also activated by DSBs, but utilizes some meiosis-specific modifications [Subramanian and Hochwagen, 2014]. Hop1 is a meiosis specific adaptor protein in place of Rad9, which when phosphorylated by Mec1/Tel1, recruits Mek1 to chromosome axes via the Mek1 FHA-domain [Carballo et al., 2008; Niu et al., 2005]. This phosphorylation allows activation of Mek1 via autophosphorylation of threonine 327 in the Mek1 activation loop [Niu et al., 2007]. Mek1 phosphorylation of substrates then ensures that DSBs are repaired in a Dmc1-dependent manner using homologs rather than sister chromatids [Niu et al., 2005; Kim et al., 2010].

There are two pathways for activating Mek1. One involves *RAD17* and the other *PCH2*, which encodes a meiosis-specific AAA+ ATpase [Ho and Burgess 2011]. Deletion of both *RAD17* and *PCH2* reduces spore viability due to a failure to efficiently repair meiotic DSBs.

Rad17 is a putative Mek1 substrate

The *dmc1Δ* mutant causes cells to arrest in meiotic prophase, due to the presence of unrepaired DSBs triggering the MRC [Bishop et al., 1992; Lydall et al., 1996]. The 3’ single

stranded ends of DSBs are unable to undergo strand invasion [Hunter and Kleckner, 2001]. Constant activity of Mek1 is required to maintain this arrest, by preventing repair of the breaks by Rad51 [Niu et al., 2007]. To get a deeper understanding of the regulation of meiotic recombination by Mek1, it is essential to identify its substrates. Previous research has identified Mek1 T327, Rad54 T132, Hed1 T40 and histone H3 T11 as four in *vivo* Mek1 substrates [Niu et al., 2007; Govin et al., 2010; Niu et al., 2009; Callender et al., 2016].

Stable Isotope Labeling by Amino acids in Cells (SILAC), is a technique developed to compare the proteomes of cells with the same genotype under different conditions. It can be coupled with phosphopeptide purification and liquid chromatography-tandem mass spectrometry (LC-MS/MS) to identify specific phosphorylation sites on proteins [Suhandynata et al., 2014]. SILAC involves growth of yeast cells in medium containing either light or heavy isotope-labeled arginine or lysine. The technique relies on cells' natural cellular metabolism to incorporate "heavy" or "light" amino acids into their proteomes, making the proteins derived from the two different media distinct in their masses, thus distinguishable using mass spectrometry (MS) [Suhandynata et al., 2014].

SILAC was used to identify potential Mek1 substrates in *dmc1Δ*-arrested cells. In addition to *dmc1Δ,* the diploid also contained *mek1-as,* which encodes an analog-sensitive version of the kinase [Wan et al., 2004]. The *mek1-as* allele contains a mutation in a single residue in the ATP binding pocket, which confers sensitivity to small molecule inhibitors [Wan et al. 2004]. The inhibitor can only bind to the mutant kinase allowing specific inactivation of the modified kinase [Wan et al., 2004]. The *dmc1Δ mek1-as* diploid was grown in both light and heavy media and the cells were transferred to a sporulation medium allowing initiation of meiosis [Suhandynata et al., 2014; Suhandynata et al., 2016].

After the cells arrested in meiotic prophase, Mek1-as inhibitor was added to the heavy culture for 20 minutes. Crude chromatin was isolated from both the heavy and light cultures and equal amounts of protein were combined and digested with trypsin to generate peptides. Using immobilized metal affinity chromatography, phosphopeptides were purified and mass spectrometry was used to identify the light/heavy (L/H) ratios of the peptides [Suhandynata et al., 2014].

Proteins that are phosphorylated by Mek1 should be under-represented in the heavy culture, thereby giving L/H ratios > 2. The approach was validated by detection of phosphopeptides with L/H ratios> 2 for two known substrates of Mek1, Mek1 T327 and Rad54 T132 [Suhandynata et al., 2014]. For analysis two data sets from the *dmc1Δ mek1-as* experiments were merged. The peptides were divided into three classes based on their L/H ratios. Those with a L/H ratio > 2 were categorized as Class 1, those with L/H ratio < 2 but > 0.5 were categorized as Class 2 and those with L/H ratio < 0.5 were categorized as Class 3 [Suhandynata et al., 2016]. The phosphopeptides were further analyzed using the Motif-X algorithm, which works by identifying phosphorylation enriched consensus motifs, and comparison of them to previously identified consensus sequences to identify which sites might be phosphorylated by Mek1 [Suhandynata et al., 2016]. Rad17 was found to have a peptide phosphorylated on T350 which exhibited an L/H ratio > 2 and was contained with the Mek1 phosphorylation site consensus sequence (RXXT), indicating it is a putative Mek1 substrate [Suhandynata et al., 2016]. The goal of my thesis was to mutate this site to determine whether phosphorylation of Rad17 during meiosis is functionally important.

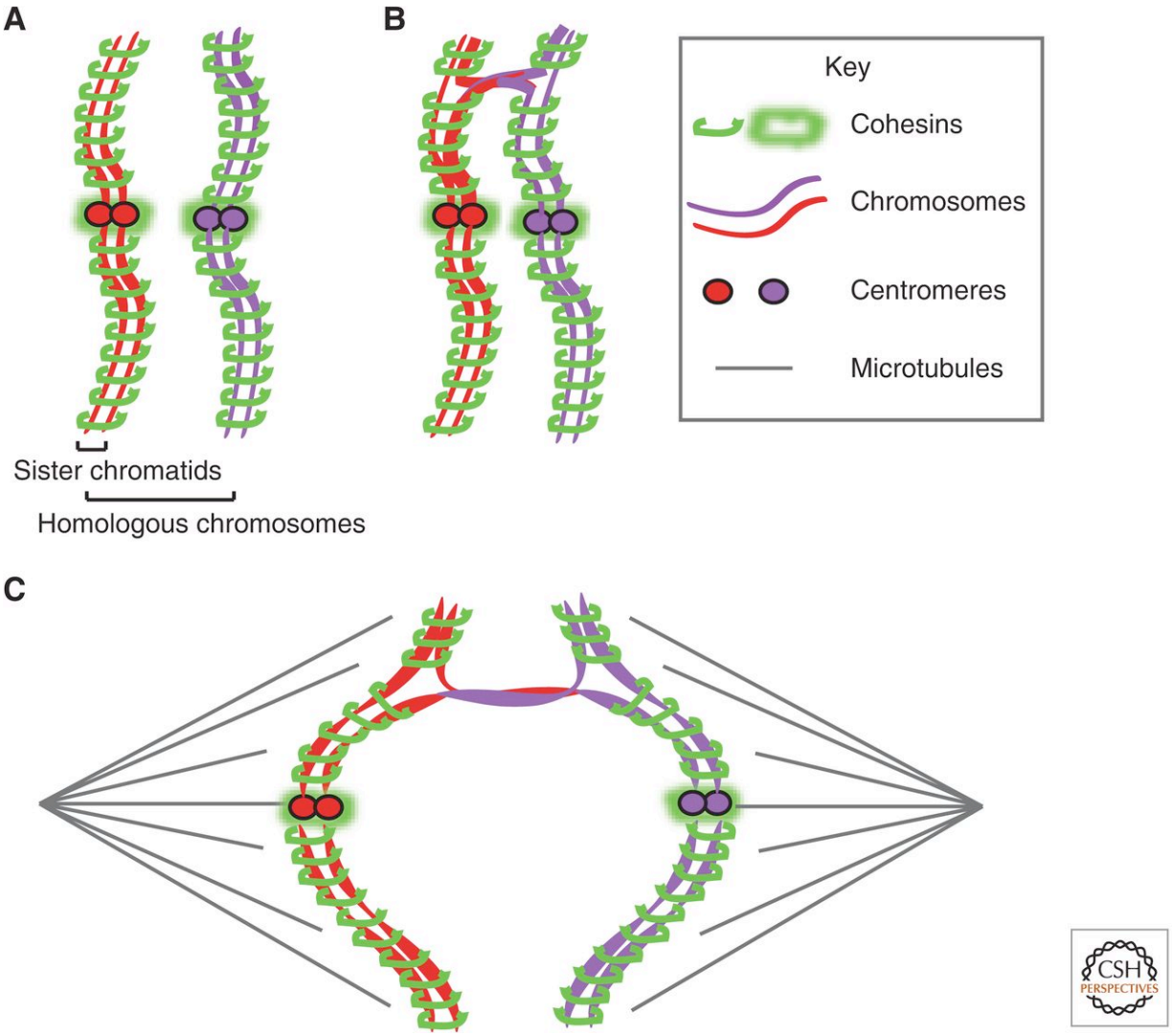

Figure 1: Crossovers and sister chromatid cohesion connect homologous chromosomes at Meiosis I (adapted from Subramanian and Hochwagen, 2014). Crossovers in combination with sister chromatid cohesion (in green, holds sister chromatids together) create physical connections between homologs, allowing them to orient properly on meiotic spindle (grey lines) during Metaphase I, thereby ensuring accurate segregation. Red and purple circles represent mono-orienting pairs of sister kinetochores.

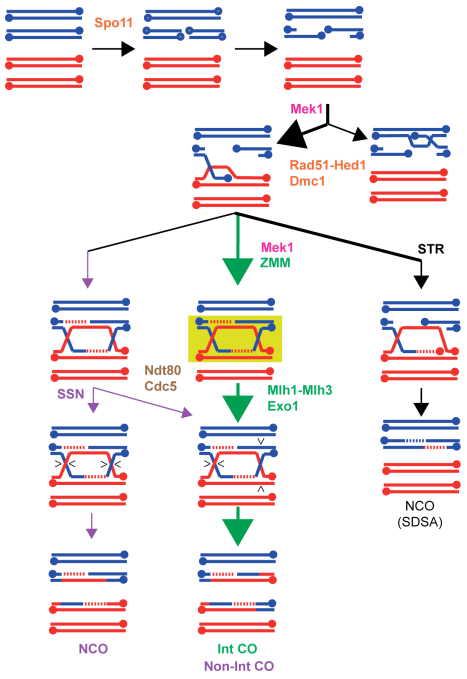

Figure 2: The double strand repair model for meiotic recombination. The red and blue lines represent the duplex DNA of homologous chromosomes. Circles indicate the 3' ends of the DNA. The meiosis-specific endonuclease, Spo11, introduces programmed DNA DSBs on one the four chromatids. 5' end resection occurs on both sides of the break, producing 3' single-strand ends. Dmc1 with the help of Rad51/Hed1 and Mek1, mediates strand invasion preferentially into the homolog. The recombination intermediates repaired via the synthesis-dependent strand annealing (SDSA) pathway produce noncrossover (NCO) products. SDSA requires the activity of the Sgs1 helicase, Top3 and Rmi1 (STR) [Kaur et al., 2015]. The strands repaired via the Mek1-regulated *ZMM* pathway, promote formation of double Holliday junctions that are resolved exclusively as crossovers (COs) that are distributed throughout the genome by interference (Int) [Allers and Lichten 2001; Chen et al., 2015]. Double Holliday junctions formed in the absence of the *ZMM* pathway are resolved in an unbiased way to produce both NCOs and non-interfering COs. (Figure courtesy of Nancy Hollingsworth).

Results and Methods

The goal of my project was to test whether substitution of T350 in *RAD17* with alanine (to prevent phosphorylation) or aspartic acid (to act as a phosphomimic) had any phenotypes in meiosis. To accomplish this goal, I made an integrating plasmid containing *RAD17* and a yeast selectable marker and introduced the T350A and T350D mutations into this plasmid. I made a *rad17Δ* diploid into which the *RAD17*, *RAD17-T350A* or *RAD17-T350D* plasmids were integrated to check for complementation of various *rad17Δ* phenotypes such as spore viability. Although I did not have time to do the phenotypic characterization of the resulting strains, Lihong Wan subsequently carried out this analysis in the Hollingsworth lab [Suhandynata et al., 2016].

Constructing a *RAD17 TRP1* integrating plasmid

The first step in creating mutations in *RAD17* was to make a *TRP1* integrating plasmid containing the *RAD17* gene. A 1687 bp fragment containing sequences between coordinates 1026563 and 1028250 on chromosome XV of *Saccharomyces cerevisiae* was synthesized by Genewiz. This fragment was engineered with 5'-SalI and 3'-BamHI ends and cloned into pUC57-Kan (pUC57-RAD17). The fragment contains the *RAD17* open reading frame (ORF) with 280 base pairs (bp) 5' to the start codon and 217 bp downstream of the stop codon. To amplify the plasmid, a maxi-prep was performed after first transforming pUC57-RAD17 into bacteria. The plasmid was diluted to a concentration of 1ng/μL in 1 mM Tris-HCL, 1 mM EDTA, pH 8 (TE) and 1 μL was added to competent DH5α bacterial cells. The cells were incubated on ice for 30 minutes, heat-shocked at 42˚C for 45 seconds, and placed back on ice for 2 minutes. 0.9 mL of pre-warmed Lysogeny Broth (LB) was added and the microfuge tubes containing the cells were taped to a roller at 37˚C for 1 hour. Both

100 µL and 500 µL cells were spread onto two LB+ 50 µg/mL Kanamycin (Kan) plates and incubated overnight at 37°C to allow growth. Ten pUC57-RAD17 transformants were observed for the LB+Kan plate with 100 µL cells and 38 pUC57-RAD17 transformants were observed with 500µL of cells.

One Kan^R transformant was inoculated into the 200 mL liquid LB + Kan in a 1 L flask and incubated on a 37°C shaker overnight. A maxi-prep was performed using the Qiagen Maxi-prep Plasmid DNA purification kit following the manufacturer's instructions. To confirm the presence of the 1.7 kb BamHI/SalI insert in the maxi-prep of pUC57-RAD17, 2 µL of 100 ng/µL pUC57-RAD17 were digested in a total of 20 µL using 1.0 µl of either BamHI, SalI, KpnI or BamHI and SalI and the DNA was fractionated using a 0.8% Tris-Borate-ethylenediaminetetraacetic acid (TBE) agarose gel at 100 V for 1 hour. 15 µL of 15 mg/mL Ethidium Bromide was added to the buffer before running the gel to enable detection of the DNA under ultraviolet (UV) light. The pUC57-RAD17 digest with BamHI or SalI alone gave one 4.2 kb fragment as expected, while the BamHI/SalI double digest exhibited two fragments of 1.7 kb and 2.5 kb (Figure 3). The KpnI enzyme did not appear to cut the plasmid. At the same time, the pRS304 *TRP1* yeast shuttle vector was digested with BamHI, SalI or EcoRI. The pRS304 digest exhibited a 4.2 kb fragment, as expected for the linearized plasmid (Figure 3).

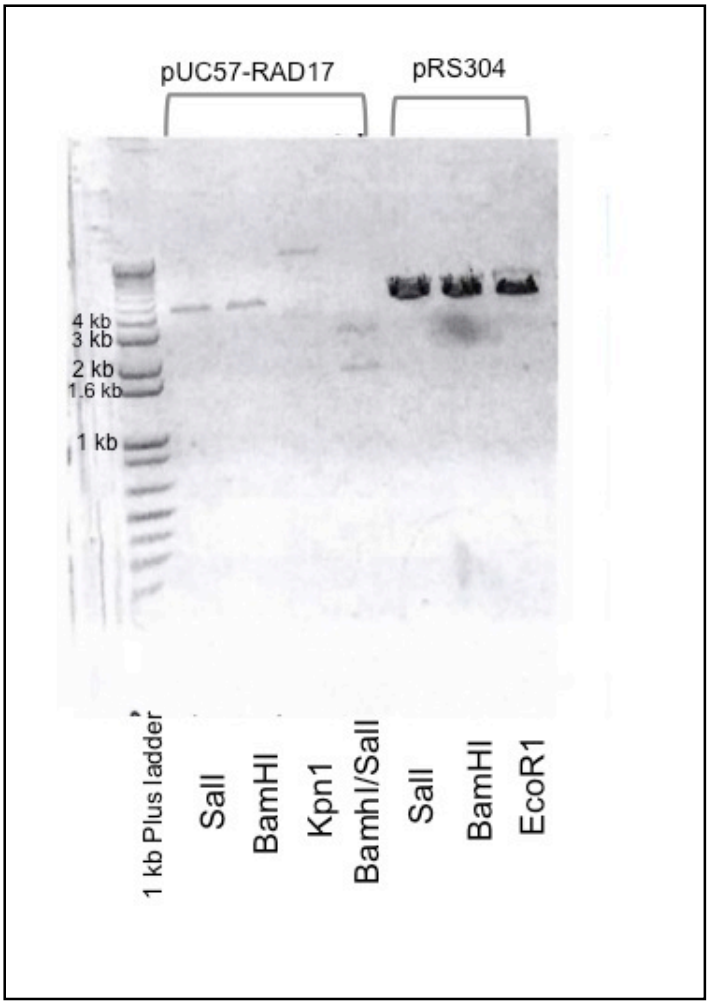

Figure 3: Restriction digest analysis for pUC57-RAD17 and pRS304. Maxi-preps of pUC57-RAD17 and pRS304 were digested with the indicated restriction enzymes, fractionated by agarose gel electrophoresis and visualized using UV light after ethidium bromide staining of the DNA. The first lane contains the 1 kb Plus ladder of DNA molecular weight markers.

Construction of pMR1: a *RAD17 TRP1* integrating plasmid

To make pMR1 (Figure 4), the 1.7 kb BamHI/SalI fragment from pUC57-RAD17 was subcloned into pRS304 digested with BamHI and SalI. The reaction tubes for both plasmids

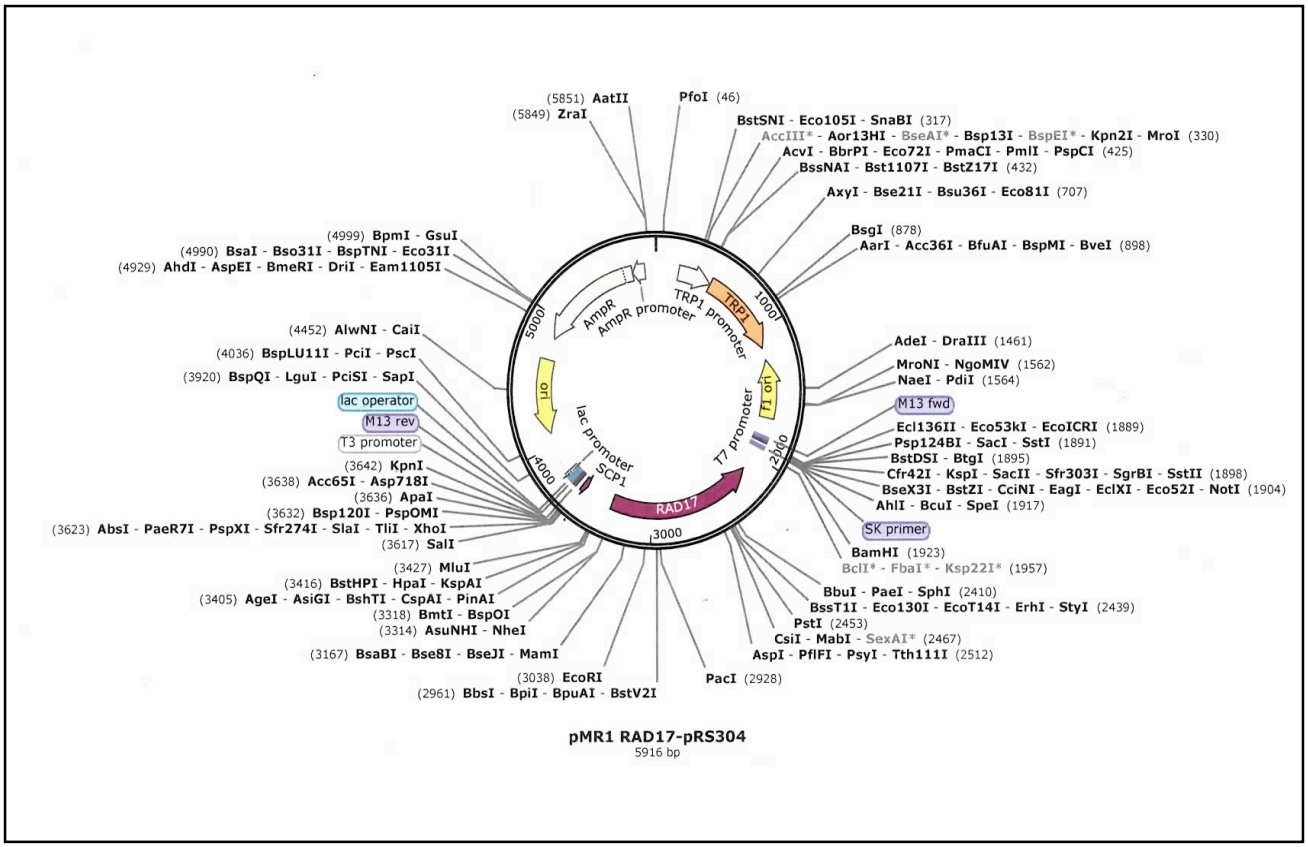

Figure 4: Restriction map of pMR1: a *RAD17 TRP1* integrating plasmid. Unique six cutters are shown in bold.

contained 5.0 µL of 10 X New England Biolab (NEB) Buffer 3, 5.0 µL of 10 X Bovine Serum Albumin (BSA), 2.0 µL of SalI, 2.0 µL of BamHI and water to a total volume of 50 µL. 5 µg of either pRS304 or pUC57-RAD17 was included in the reaction. The digests were incubated for four and a half hours at 37˚C. To purify the 1.7 kb BamHI/SalI fragment from pUC57-RAD17 and the BamHI/SalI linearized pRS304 vector, 10 µL of 6 X DNA sample buffer was added to both digests and the DNA was loaded onto a 0.8% Tris-acetate Ethylenediaminetetraacetic (TAE) agarose gel and allowed to run at 80 V for 1 hour.

Ethidium Bromide was added to the buffer before running the gel, which allowed for observing the DNA under UV light. A hand-held low wave UV lamp was used to visualize the bands and the 1.7 kb BamHI/SalI fragment from the pUC57-RAD17 and the 4.2 kb pRS304 BamHI/SalI vector fragment were cut out. The fragments were purified from the agarose using the Qiagen Mini-Prep purification kit and the DNA for was eluted in 30 µL WATER. A Nanodrop spectrophotometer was used to quantify the DNA. The concentration of the 1.7 kb BamHI/SalI fragment was 5.6 ng/µL and the pRS304 BamHI/SalI fragment was 10 ng/µL.

For the ligation reaction, control and experimental reactions were set up. Each 20 µL reaction contained 1 µL of 10 ng pRS304/BamHI/SalI-digested vector, 2 µL of 10 X T4 DNA ligase buffer, 1 µL of T4 ligase. The ligation control tube contained no 1.7 kb insert and 16 µL of water while the experimental ligation (pMR1) contained 9.0 µL of 5.6 ng 1.7 kb *RAD17*/BamHI/SalI fragment and 7 µL of water. The contents of the tubes were mixed, centrifuged and incubated at room temperature for 30 minutes.

For transformation, two tubes of frozen competent DH5α cells were thawed on ice for 10 minutes. To one tube, 4 µL of the control reaction was added, while 4 µL of the pMR1 ligation were added to the other tube. The cells were incubated on ice for 30 minutes, followed by heat shock at 42˚C for 45 seconds. The tubes were placed back on ice for 2 minutes after which 0.9 mL pre-warmed LB was added and the tubes were incubated by taping the microfuge tubes to a roller at 37˚C for 1 hour .The cells were spread on LB+100 µg/mL Ampicillin (Amp) plates and incubated at 37˚C overnight. Since the single strand DNA ends generated by BamHI and SalI contain different sequences, the two ends of the pRS304 vector cannot anneal and therefore no transformants should have been observed if

digestion of the plasmid was complete. This was the case as there were 0 transformants with the control reaction. In contrast, 25 colonies were observed for one pMR1 ligation containing both vector and insert and 15 colonies observed for a second pMR1 ligation. These colonies should contain both the vector with the insert since they grew on LB+Amp plates. The vector contains the gene for resistance to ampicillin as well as a bacterial origin of replication (Figure 4), while the insert contains the ends compatible with the BamHI and SalI cut ends of the vector, allowing them to anneal, thus allowing formation of a circular plasmid. The next morning, DNA from six of the pMR1 transformants was purified using the Qiagen mini-prep purification kit. The presence of the insert was confirmed using restriction digest analysis. The reactions contained 2 µL mini-prep DNA from candidate pMR1 plasmids, 1 µL SalI, 1 µL BamHI, 2 µL 10 X NEB buffer 3, 2 µL 10 X BSA and 12 µL WATER. The digests were incubated at 37˚C for 1 hour. 4 µL of 6 X DNA sample buffer were added and the DNA was loaded onto a 0.8% TBE agarose gel and allowed to run at 100V for 1 hour. BamHI/SalI digested pRS304 and pUC57-RAD17 were included on the gel as controls. Ethidium Bromide was added to the buffer before running the gel, which allowed detection of the DNA under UV light. The presence of the 1.7 kb insert containing *RAD17* and 4.2 kb vector fragment confirmed that all of plasmids were correct (Figure 5). pMR1 mini-prep 3 was selected and purified using the Qiagen Maxi-prep Plasmid DNA purification kit following the manufacturer's instructions. A Nanodrop spectrophotometer was used to quantify the DNA. The concentration of the pMR1 was 93.5 ng/µL.

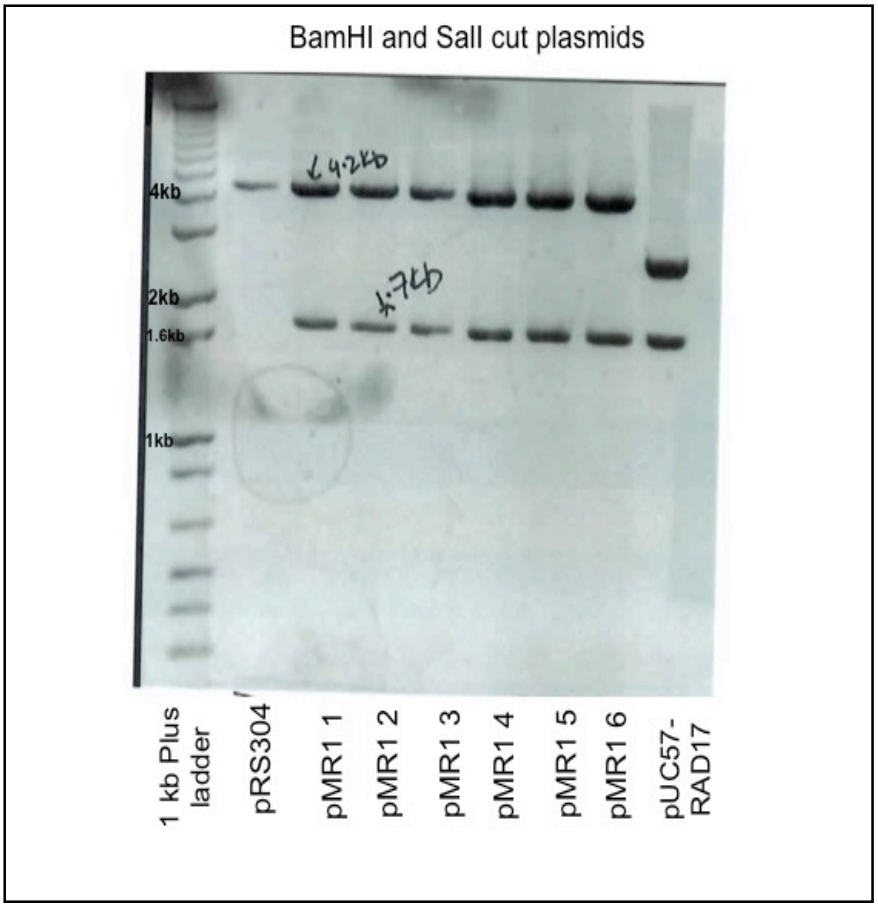

Figure 5: Digestion of pMR1 mini-prep DNA with BamHI and SalI to check for the presence of the 1.7 kb insert containing *RAD17.*

Site directed mutagenesis:

For site directed mutagenesis, the potential Mek1 phosphorylation site in *RAD17* is the codon-specifying threonine at position 350 (ACA). This codon was changed to aspartic acid (GAT) or alanine (GCA) (Figure 6). For the mutagenesis reaction, the melting temperatures of the mutagenic primers was determined using the following formulation:

$$T_m = 81.5 + 0.41\ (\%GC) - (675/N) - \%\ \text{mismatch};$$

N is the primer length in bases, and values for % GC and % mismatch are whole numbers. Ideally, the melting temperature of the primers should be ≥ 78˚C. RAD17-T350D-F had 12% GC content, 6% mismatch giving a T_m of 74.5˚, and RAD17-T350D-F-r had 14% GC content, 4% mismatch giving T_m of 78.9˚. T_m for RAD17-T350A-F was 79.2˚ with 13% GC content and 2% mismatch while T_m for RAD17-T350A-F-r was 74.5˚ with 12% GC content and 6% mismatch.

For the mutagenesis, two polymerase chain reactions (PCR) were set up such that both reaction tubes contained 5.0 µL of 10 X Pfu Turbo reaction buffer, 1.0 µL of 50 ng/µL pMR1, 5 µL 2 mM deoxyribonucleotide triphosphates (dNTPs) and 29 µL of water. For the T350D mutagenesis, the reaction contained 5.0 µL each 25 ng/µL of RAD17 T-350D-F and RAD17 T-350D-F-r. For the T350A mutagenesis, the reaction tube contained 5.0 µL each 25 ng/µL RAD17 T-350A-F and RAD17 T-350A-F-r. The contents of the reaction tubes were mixed well and put into the PCR machine. The PCR conditions were: 95˚C for 30 seconds, [denaturing step 95˚C for 30 seconds, annealing step 55˚C for 1 minute, Extension step 68˚C for 1 minute]. The steps in brackets were repeated for 18 cycles. 5.0 µL from each reaction was transferred to a new tube and 1.0 µL 6X sample buffer was added and the sample run on a 0.8% TBE agarose gel at 100V for 1 hour. Ethidium Bromide was added to the buffer,

which allowed for the bands to be observed under UV light (Figure 7).

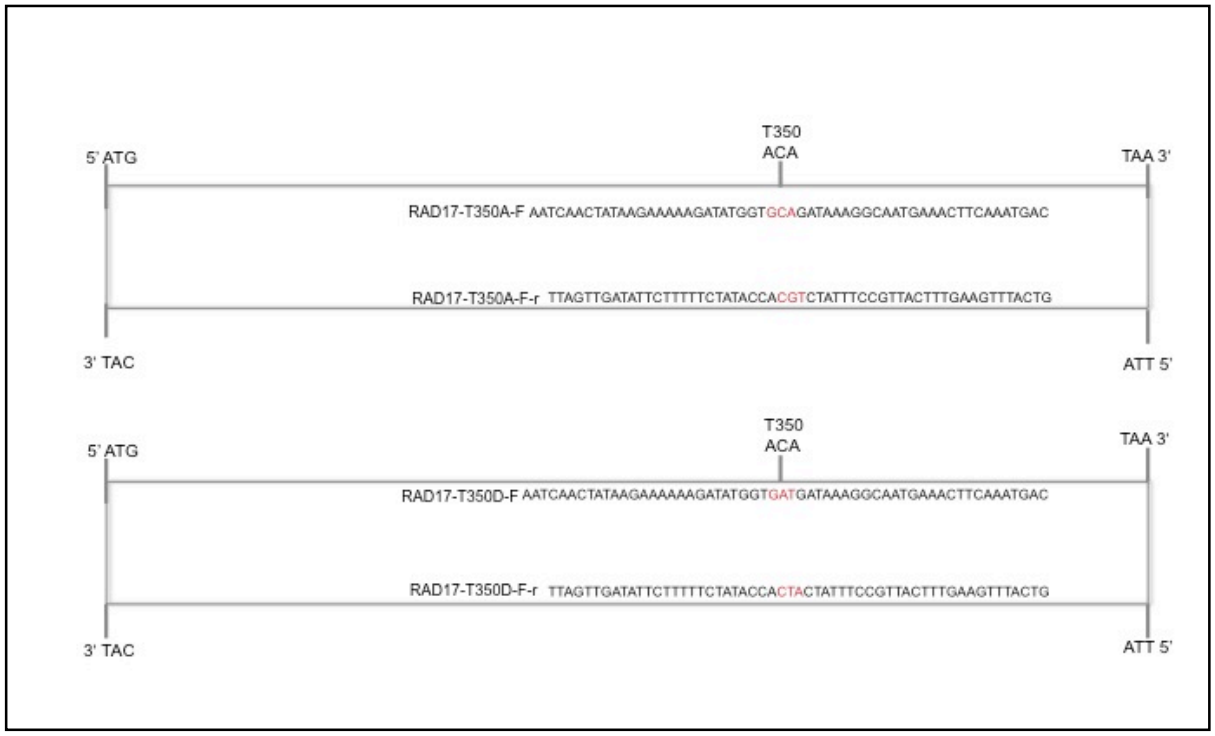

Figure 6: Primers used to mutate the *RAD17* T350 ACA codon to either an alanine codon (GCA) or an aspartic acid codon (GAT).

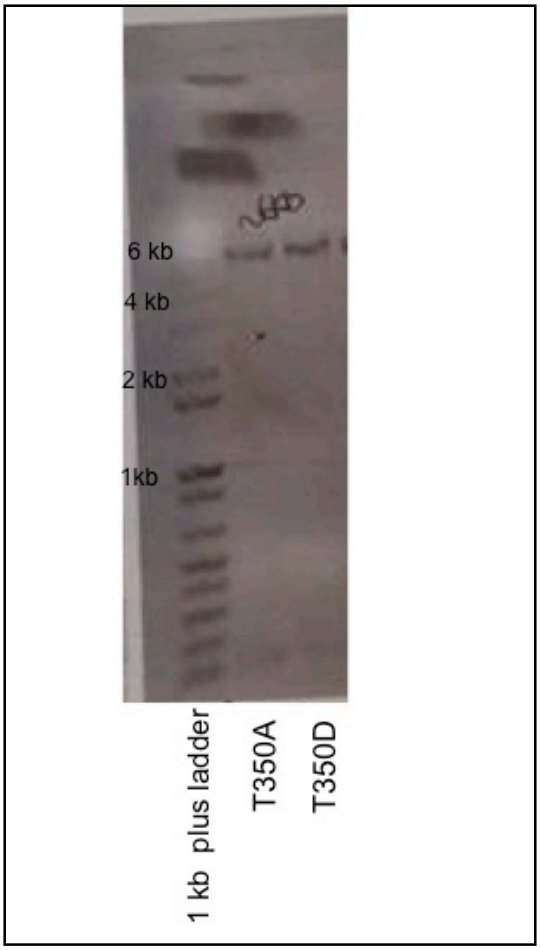

Figure 7: PCR amplification of pMR1 using primers that change the *RAD17* T350 codon to specify either alanine or aspartic acid. The expected size of the linear pMR1 PCR product is ~6 kb.

The PCR products were treated with the restriction enzyme Dpn1, which digests parental methylated and hemi-methylated DNA and then transformed into DH5α cells and spread on LB+Amp plates, which were incubated at 37˚C overnight. 81 colonies were observed for T350A plasmid tranformation and 59 colonies were observed for T350D plasmid transformation. Three colonies from each plate were inoculated into 4 mL of LB+AMP and incubated overnight at 37˚C on a roller. The Qiagen mini-prep purification kit was used to purify the plasmids. To see if the plasmids contained the appropriate mutation, 3 μl of 100 ng/μl of mini-prep DNA was combined with 1 μl 3.2 μM RAD17-SEQ3 and 8μL water in a 0.2 ml PCR and sent to the Stony Brook University Sequencing Facility. RAD17-SEQ3 is a forward primer, oriented 240 bp upstream of the 350 codon mutation. All of the sequenced plasmids contained the mutations. The pMR1 plasmid with the aspartate mutation was named pMR1-T350D and the one with the alanine mutation was named pMR1-T350A. To ensure that no unwanted mutations were introduced by the PCR reactions, the *RAD17* alleles of pMR1-T350A and pMR1-T350D were sequenced in their entirety using four different primers, RAD17-SEQ-1 (a forward primer oriented 360 bp upstream of the *RAD17* start site), RAD17-SEQ-2 (a forward primer located 753 bp upstream of the 350 codon), RAD17-SEQ-5 (a reverse primer located 90 bp downstream of the 350 codon) and the M13 forward primer (also oriented downstream of the *RAD17* ORF). The full length sequencing results confirmed that the only desired T350 mutation was present.

Making a diploid homozygous for *rad17Δ::natMX4*

To make a diploid homozygous for *rad17Δ::natMX4*, the *RAD17* ORF was first substituted with the *natMX4* gene in two haploid yeast strains, NHY1210 trp1 (*MATa*

leu2::hisG HIS4::LEU2-(Bam+ori) ho::hisG ura3 (ΔSma-Pst) trp1-5'Δ::hphMX4) and NHY1215 trp1 XC (*MATα leu2::hisG his4-X::LEU2-(NgoMIV+ori) ho::hisG ura3 (ΔSma-Pst) trp1-5'Δ::hphMX4*) . *natMX4* confers resistance to antibiotic nourseothricin (NAT). The *natMX4* gene flanked by homology immediately upstream and downstream of the *RAD17* ORF was amplified using PCR (Figure 8A). The RAD17-NAT-F1 primer contains 55 bp immediately 5' of the *RAD17* ATG fused with 5'ACATGGAGGCCCAGAATACCC3' which hybridizes to DNA flanking the 5' end of *natMX4* in the plasmid p4339. RAD17-NAT-R1 contains the reverse complement of the 55 nucleotides 3' to the *RAD17* stop codon fused with 5'CAGTATAGCGACCAGCATTCAC 3', which anneals to the DNA flanking the 3' end of the *natMX4* gene. The primers were each diluted to a final concentration of 10 pmol/µl and the template plasmid p4339 was diluted to a final concentration of 40 ng/µl.

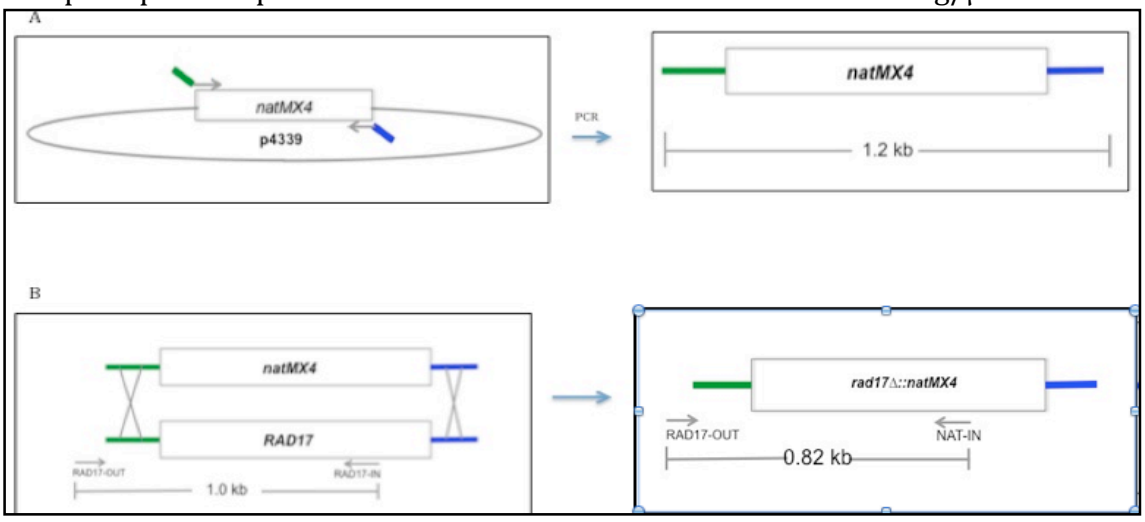

Figure 8: Strategy for making a *rad17Δ::natMX4* allele. A. A 1.2 kb *natMX4* fragment containing 55 bp of homology flanking the *RAD17* ORF was generated using p4339 and the RAD17-NAT-F1 and RAD17-NAT-R1 primers. B. Transformation of a haploid *RAD17* yeast strain with the 1.2 kb PCR fragment enables recombination to replace the *RAD17* gene with *natMX4*. The RAD17-OUT and RAD17-IN primers used to detect a 1.0 kb fragment indicative of the *RAD17* gene, while the *rad17Δ::natMX4* allele was detected using RAD17-OUT and NAT-IN to produce a 0.8 kb fragment.

Four reaction tubes were set up containing 1.0 µl 40 ng/µL p4339, 10.0 µL of 10 X ThermoPol buffer, 10.0 µL of 2 mM dNTPs, 5.0 µL 10 µM RAD17-NAT-F1, 5.0 µL 10 µM RAD17-NAT-R1, 5.0 µL of dimethyl sulfoxide, 63.0 µL WATER and 1.0 µL of Vent polymerase. The contents of the reaction tubes were mixed well before starting the PCR reaction. The PCR conditions were: 94˚C for 5 minutes, (denaturing step at 94˚C for 30 seconds, annealing step at 55˚C for 30 seconds, extension step at 72˚ for 1 minute). The steps in brackets were repeated for 25 cycles. To determine whether successful amplification occurred, 1.0 µL from each reaction was mixed with 1.0 µL 6 X buffer and 8 µL TE and run on a 0.8% TBE agarose gel at 100 V for 1 hour. Ethidium Bromide was added to the buffer before running the gel, which allowed for observing the DNA under UV light. The expected 1.2 kb fragment was observed in all of the reactions (Figure 9).

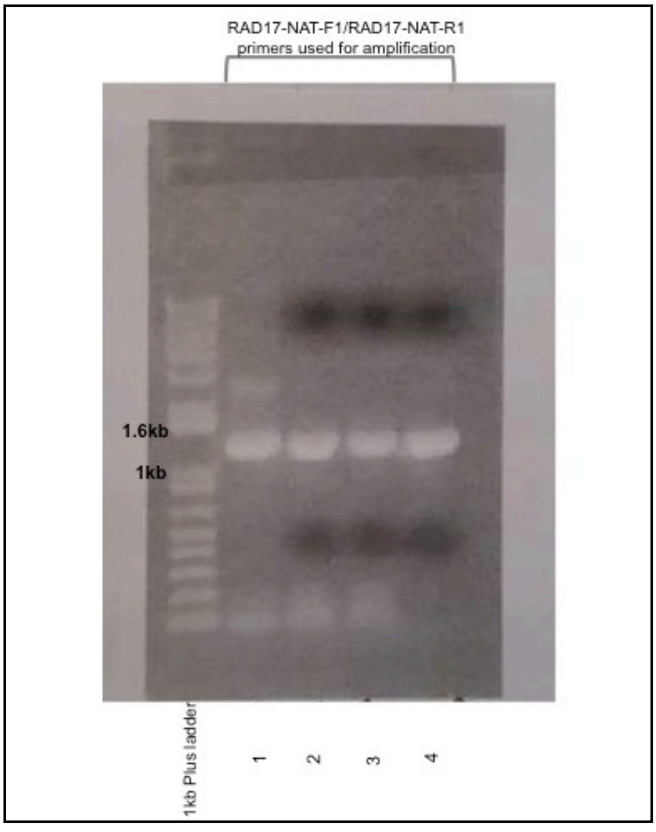

Figure 9: PCR amplification of the 1.2 kb *rad17Δ::natMX4*

To concentrate the 1.2 kb PCR fragment, the PCR reactions were pooled (400µL) in a two ml microfuge tube and precipitated by the addition of 40 µL of 3M Sodium Acetate pH 5.2, and 1.2 mL Ethanol (EtOH). The DNA was pelleted by centrifugation in a microcentrifuge at 13,000 revolutions per minute (rpm) for 10 minutes. The supernatant was discarded and 1 mL cold 70% EtOH was added and poured off. The pellet was centrifuged again and excess EtOH removed using a pipetteman. After the pellet was air dried, the DNA was resuspended in 45 µL TE buffer.

NHY1210 trp1 and NHY1215 trp1 XC were then transformed with the 1.2 kb *rad17Δ::natMX4* fragment. A single colony from each strain was inoculated into two mL of yeast extract peptone dextrose medium (YPD). Part of the colony was patched onto glycerol as non-fermentable carbon source to make sure the cells were not petite (i.e. they have mitochondrial function, since glycerol requires respiratory growth). The cultures were grown for approximately 24 hours on a roller at 30˚C. The cultures were diluted 1:50 into 100 mL of YPD in 250 ml flasks, and allowed to grow for an additional 4-5 hours at 30˚C while shaking. The cells were pelleted in a Sorvall centrifuge using a GSA rotor at 5000 rpm for 10 minutes. The supernatants were discarded and the cell pellets were resuspended in 10 mL water and transferred to sterile glass test tubes. The cells were then pelleted by centrifugation using a tabletop centrifuge at setting 5 for 5 minutes. The supernatants were discarded and cells were resuspended in 0.5 mL of 1M LiOAc-TE solution (0.3 mL of 1M LiOAc pH 7.5 + 0.3 mL 10 X TE pH 7.5 + 2.4 mL water).

For each strain three transformation tubes were set up in 1.5 mL microfuge tubes. Each transformation contained 100 µL of cells and 10 µL of 10 mg/mL single strand carrier DNA. The carrier DNA was placed at 95˚C for five minutes to allow denaturing before

aliquoting it into the tubes. One tube contained 0 µL of DNA. No transformants should be observed for this plate, since it lacks the *rad17Δ::natMX4* fragment which carries resistance to NAT. The other two transformations contained 10 µL of 1.2 kb *rad17Δ::natMX4* fragment. To each tube, 0.7 mL of 100 mM LiOAc-40% Polyethylene glycol (PEG) [0.5mL 1M LiOAc pH 7.5 + 0.5mL 10 X TE + 4.0mL 50% PEG] was added. The cells were then incubated at 30˚C for 30 minutes, followed by heat shock at 42˚C for 15 minutes. The cells were then pelleted at 13,000 rpm for 1 minute. The supernatants were discarded and the cells were resuspended in 0.5 mL of YPD. The resuspended pellet was added to a test tube containing 2 mL of YPD and placed on a roller for 1 hour to give the cells a chance to transcribe the *natMX4* gene and translate the RNA into protein so that the *natMX4* gene product is present to inactivate the NAT when plated on the drug. The cells were then plated on YPD+ 100 µg/mL NAT plates. The plates were incubated at 30˚C for 3 days.

No transformants were observed for the control plate containing no DNA. 25 transformants were observed for NHY1210 trp1 and 13 transformants were observed for NHY 1215 trp1 XC. The transformants were replica plated onto YP+2% Glycerol, NAT and 30 µg/mL HygB plates. They were replicated to YP +glycerol to ensure that the transformants were not petite. Because the *hphMX4* and *natMX4* genes are flanked by the same homology, recombination can occur between the *natMX4* fragment and the *hphMX4* gene that was used partially delete *TRP1* on the chromosome. It was therefore necessary to confirm that the NatR transformants still contained the hphMX4 gene by confirming that they were still resistant to HygB. Out of 25 colonies examined for NHY1210 trp1, 17 colonies grew on 30 µg/mL HygB while only 14 grew on YP+glycerol plate; 3 colonies did not grow on either glycerol and HygB plates. For NHY1215 trp1 XC, 12 out of 13 colonies

grew on HygB while only 8 grew on YP+glycerol plate; 1 colony did not grow on glycerol and HygB plates. Colonies that grew on all three media were selected for the colony PCR.

To determine whether the Nat^R transformants were deleted for *RAD17*, colony PCR was used to test for the presence of the *rad17Δ::natMX4* allele, as well as the absence of the *RAD17* allele. A crude preparation of yeast DNA was generated from seven freshly grown Nat^R transformants from both NHY1210 trp1 and NHY1215 trp1 XC. A pipetman tip was used to transfer a small part of the patch into 30 µL of 0.2% sodium dodecyl sulfate (SDS). The cells were vortexed for 15 seconds, heated at 95˚C for 4 minutes and then pelleted by microcentrifugation for 1 minute. The supernatants containing the DNA were transferred to new tubes. Two 50 µL PCR reactions were set up such that each reaction tube contained 5.0 µL 10 X Choice Taq buffer, 2.0 µL 25% Triton X-100, 5.0 µL 2mM dNTPs, 29.5µL water, 0.5µL Taq polymerase and 2.5µL of 10 pmol/µL of RAD17-OUT. One reaction contained 2.5 µL of 10 pmol/µL RAD17-IN (to detect a 1 kb fragment indicative of the *RAD17* gene), while the other contained 2.5 µL of 10 pmol/µL NAT-IN (to detect a 0.82 kb fragment indicative of *rad17Δ::natMX4*) (Figure 8).

The contents of the reaction tubes were mixed well before starting the PCR reaction. The PCR conditions were as follow: 95˚C for 1 minute (denaturing step at 95˚ for 30 seconds, annealing step at 54˚C for 1 minute, extension step at 72˚C for 1 minute), 72˚C for 6 minutes. The steps in brackets were repeated for 35 cycles. 10.0 µL of 6 X buffer was added to each PCR reaction and 15.0 µL was run on a 0.8% TBE agarose gel at 100 V for 1 hour. Ethidium Bromide was added to the buffer before running the gel, which allowed for detection of the the DNA under UV light (Figure 10). All the transformants contained the

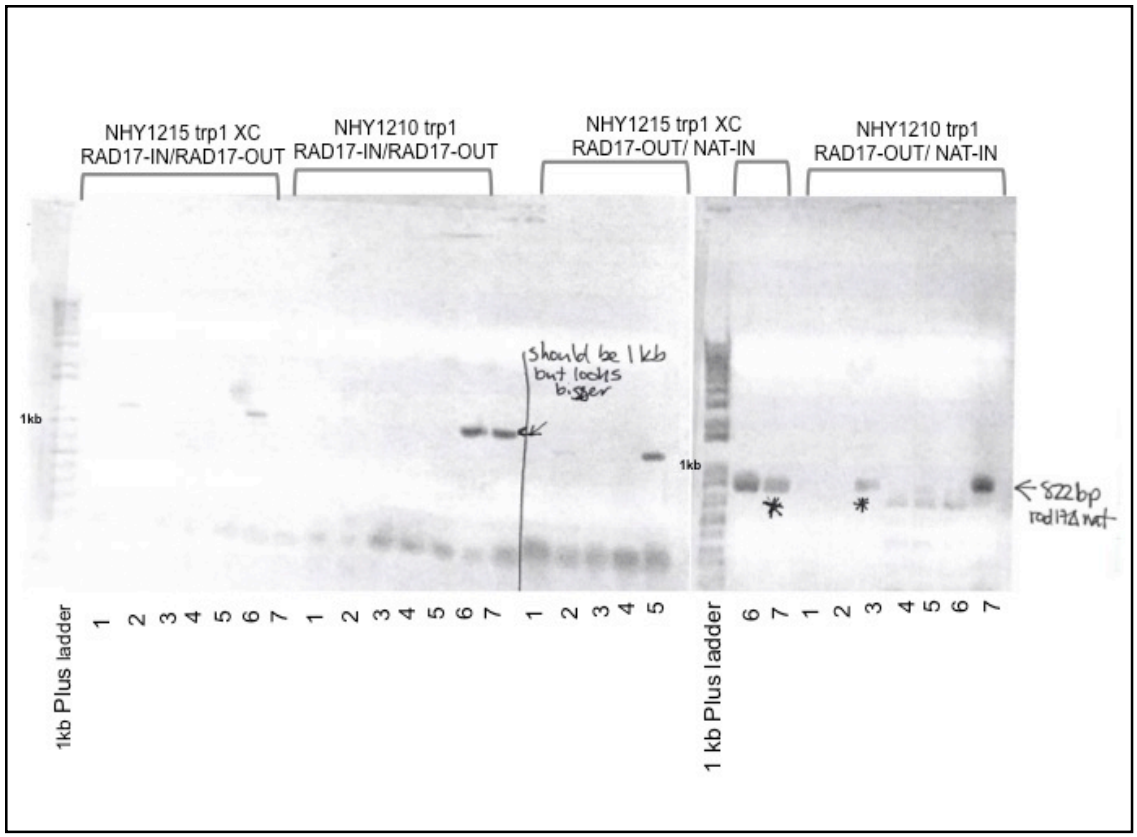

Figure 10: Using colony PCR to verify the genotype of NHY1210 trp rad17 and NHY1215 trp1 XC rad17. The predicted size for the RAD17 allele using the RAD17-OUT and RAD17-IN primers is 1.0 kb, while the size of the fragment using RAD17-OUT and NAT-IN is 0.8 kb. Transformant number 3 was selected for NHY1210 trp1, and transformant number 7 was selected for NHY1215 trp1 XC since both of them gave the predicted 0.8kb RAD17-OUT and NAT-IN fragment and lacked the 1kb RAD17 allele.

natMX4 gene, which allowed them to grow on NAT plates. To ensure that the *natMX4* was incorporated in place of *RAD17*, colony PCR products fragments on the agarose gel were examined. Transformant number 3 was selected for NHY1210 trp1, and transformant number 7 was selected for NHY1215 trp1 XC since they both gave the predicted 0.8 kb fragment with RAD17-OUT and NAT-IN and did not give the 1kb WT RAD17 allele with

RAD17-IN and RAD17-OUT. These transformants containing the *rad17Δ::natMX4* allelewere named NHY1210 trp1 rad17, and NHY1215 trp1 XC rad17 and frozen down at -80˚C.

Construction of rad17Δ diploid:

To make the NH2341 diploid, NHY1210 trp1 rad17 and NHY1215 trp1 XC rad17 were mated on YPD plates by mixing the cells together and then incubating them overnight at 30˚C. Mating patches were replica plated to synthetic dextrose (SD) medium lacking histidine (SD-His) plates. NHY1210 trp1 rad17 is prototrophic for histidine while NHY1215 trp1 XC rad17 is auxotrophic for histidine and both strains contained a mutation in ura3. Colonies grown on YPD are a mix of haploids of both strains as well as diploids. The NHY1215 trp1 XC rad17 haploid cannot grow on SD-His, so the resulting His^+ patch will contain both diploid cells which are heterozygous for *HIS4* and therefore can grow without histidine and NHY1210 trp1 rad17 haploid cells. . To isolate a NH2341 diploid colony, cells from the mating were streaked out for single colonies on YPD. Single colonies were patched out on YPD. In addition, mating type tests was performed by crossing each patch to *MATa lys1* and *MATα lys1* tester strains. Colonies are formed only after successful mating between opposite mating types and complementation of auxotrophies allows growth on SD plates. A diploid of NHY1210 trp1 rad17, and NHY1215 trp1 XC rad17 would thus not grow on SD plate, due to the presence of mutant ura3.

Haploids can mate but cannot sporulate on Spo plates; while diploid cannot mate but can sporulate on Spo plates. The diploid created by the cross between NHY1210 trp1 rad17 and NHY1215 trp1 XC rad17 would thus sporulate on Spo plate. A non-mating patch (hence a diploid) that did not grow on SD plates after being crossed to the mating tester

strains but sporulated on a Spo plate was picked and named NHY2341. Part of the patch was inoculated into 2 mL of YPD and placed on a roller at 30˚C overnight. 1 mL of NHY2341 and 1mL of 50% glycerol were added to a vial, vortexed and frozen at -80˚C .

Discussion:

I constructed the *rad17Δ* diploid as well as the plasmids, pMR1-T350D and pMR10T350A, but unfortunately did not have time to test the *rad17* mutants on these plasmids for complementation of *rad17Δ* phenotypes. However, subsequent studies done by Lihong Wan and Nancy Hollingsworth tested for the functionality of Rad17 T350 phosphorylation site *in vivo* by looking at spore viability. While a modest reduction in spore viability was observed for both *rad17-T350A* and *rad17-T350D,* the difference was not significant (unpaired T-test with Welch correction, P=0.189) [Suhandynata et al., 2016]. Deletion of *Rad17* has previously been associated with a further decrease in spore viability when combined other mutants. They introduced mutants of different genes such as *PCH2*, a AAA+ATPase involved in regulating Hop1 levels, *NDJ1*, gene required for promoting homolog pairing, and a *ZIP1*, which encodes the transverse filament protein of the synaptonemal complex in yeast [Börner et al., 2008; Wanat et. al., 2008; Wu et al., 2006] (Dong and Roeder et al., 2000). Plasmids containing *RAD17, rad17-T350A* or *rad17-T350D* were introduced into the appropriate double mutants and assayed for sporulation and spore viability. Both *rad17-T350A* and *rad17-T350D* complemented sporulation and spore viability defects of rad1*7Δ* in the *pch2Δ* and *zip1Δ* backgrounds [Suhandynata et al., 2016]. They observed a small reduction in sporulation and spore viability for *zip1-T350A* in the *ndj1Δ* background, but it was not clear whether the difference was significant [Suhandynata et al., 2016]. This led the authors to conclude that the phosphorylation of

putative Mek1 dependent phosphosite on Rad17 is not required for the primary function of *RAD17* during meiosis but could have other functions [Suhandynata et al., 2016]. Thus more work is required to determine the functional importance of Rad17 T350 phosphorylation.

References:

Allers T, Lichten M. Differential timing and control of noncrossover and crossover recombination during meiosis. Cell. 2001;106(1):47–57. PMID:11461701. doi: 10.1016/s0092-8674(01)00416-0

Bishop DK, Park D, Xu L, Kleckner N. *DMC1*: a meiosis-specific yeast homolog of *E. coli recA* required for recombination, synaptonemal complex formation and cell cycle progression. Cell. 1992; 69:439–56. pmid:1581960 doi: 10.1016/0092-8674(92)90446-j

Bishop DK. RecA homologs Dmc1 and Rad51 interact to form multiple nuclear complexes prior to meiotic chromosome synapsis. Cell. 1994;79:1081–92. pmid:7528104 doi: 10.1016/0092-8674(94)90038-8

Borner GV, Barot A, Kleckner N. Yeast Pch2 promotes domainal axis organization, timely recombination progression, and arrest of defective recombinosomes during meiosis. Proc Nat Acad Sci USA. 2008;105(9):3327–32. Epub 2008/02/29. doi: 10.1073/pnas.0711864105 pmid:18305165; PubMed Central PMCID: PMC2265181.

Borner GV, Kleckner N, Hunter N. Crossover/noncrossover differentiation, synaptonemal complex formation, and regulatory surveillance at the leptotene/zygotene transition of meiosis. Cell. 2004;117(1):29–45. Epub 2004/04/07. PMID:15066280. doi: 10.1016/s0092-8674(04)00292-2

Brown M.S, Grubb J, Zhang A, Rust J, Bishop K. Small Rad51 and Dmc1 complexes often co-occupy both ends of a meiotic DNA double strand break PLoS Genetics 2015. doi: 10.1371/journal.pgen.1005653

Buonomo SB, Clyne RK, Fuchs J, Loidl J, Uhlmann F, Nasmyth K. Disjunction of homologous chromosomes in meiosis I depends on proteolytic cleavage of the meiotic cohesin Rec8 by separin. Cell. 2000;103:387–398.

Callender TL, Laureau R, Wan L, Chen X, Sandhu R, Laljee S, Zhou S, Suhandynata RT, Prugar E, Gaines WA, Kwon Y, Borner GV, Nicolas A, Neiman AM, Hollingsworth NM. Mek1 down regulates Rad51 activity during yeast meiosis by phosphorylation of Hed1. PLOS Genetics. 2016; doi.org/10.1371/journal.pgen.1006226

Carballo JA, Johnson AL, Sedgwick SG, Cha RS. Phosphorylation of the axial element protein Hop1 by Mec1/Tel1 ensures meiotic interhomolog recombination. Cell. 2008;132:758–70. doi: 10.1016/j.cell.2008.01.035. PMID:18329363

Chen X, Suhandynata RT, Sandhu R, Rockmill B, Mohibullah N, Niu H, et al. (2015) Phosphorylation of the Synaptonemal Complex Protein Zip1 Regulates the Crossover/Noncrossover Decision during Yeast Meiosis. PLoS Biol 13(12): e1002329. doi:10.1371/journal.pbio.1002329

De Muyt A, Jessop L, Kolar E, Sourirajan A, Chen J, Dayani Y, Lichten M. BLM helicase ortholog Sgs1 is a central regulator of meiotic recombination intermediate metabolism. Mol Cell 2012; 46: 43-53. pmid:22500736, doi: 10.0116/j.molcel.2012.02.020

Dong H, Roeder GS. Organization of the yeast Zip1 protein within the central region of the synaptonemal complex. J Cell Biol. 2000;148(3):417–26. Epub 2000/02/09. pmid:10662769; PubMed Central PMCID: PMC2174805.

Game JC, Zamb TJ, Braun RJ, Resnick M, Roth RM. The role of radiation (rad) Genes in Meiotic Recombination in Yeast. Genetics 1980. PMC 1214137

Gergan J., Zhang C., Rumpf C., Cipak L., Li Z., Uluocak P., Nasmyth K., Shokat KM., 2010. Construction of conditional analog-sensitive kinase alleles in the fission yeast *Schizosaccharomyces pombe*. Europe PubMed Central. doi:10.1038/inprot.2007.447 PMCID: PMC2957860.

Gobbini E, Cesena D, Galbiati A, Lockhart A, Longhese MP. Interplays between ATM/Tel1 and ATR/Mec1 in sensing and signaling DNA double-strand breaks. DNA repair (Amst). 2013;12(10):791–9. doi: 10.1016/j.dnarep.2013.07.009 PMID:23953933

Govin J, Dorsey J, Gaucher J, Rousseaux S, Khochbin S, Berger SL. Systematic screen reveals new functional dynamics of histones H3 and H4 during gametogenesis. Genes Dev. 2010;24(16):1772–86. doi: 10.1101/gad.1954910 pmid:20713519; PubMed Central PMCID: PMC2922505.

Hassold T, Hunt P. To err (meiotically) is human: the genesis of human aneuploidy. Nature Rev. Genet. 2001;2:280–291. PMID:11283700. doi: 19.1038/35066065

Henry JM, Camahort R, Rice DA, Florens L, Swanson SK, Washburn MP, Gerton JL. Mnd1/Hop2 facilitates Dmc1-Dependent interhomolog crossover formation in Meiosis of Budding Yeast. Mol Cell Biol. 2006 Apr;26(8):2913-23.pmid:1658176, doi: 10.1128/MCB.26.8.2913-2923.2006

Ho HC, Burgess SM. Pch2 acts through Xrs2 and Tel1/ATM to modulate interhomolog bias and checkpoint function during meiosis. PLoS Genet. 2011;7(11):e1002351. Epub 2011/11/11. doi: 10.1371/journal.pgen.1002351 pmid:22072981; PubMed Central PMCID: PMC3207854.

Hollingsworth NM. Mek1/Mre4 is a master regulator of meiotic recombination in budding yeast. Microbial Cell. 2016;3(3):129–31. doi: 10.15698/mic2016.03.487

Hollingsworth NM., Ponte L., Halsey C. *MSH5*, a novel MutS homolog, facilitates meiotic reciprocal recombination between homologs in *Saccharomyces cerevisiae* but not in mismatch repair. Genes and Development 1995 9: 1728-1739

Hoque, M.T and Ishikawa, F. Cohesin defects lead to premature sister chromatid separation, kinetochore dysfunction, and spindle-assembly checkpoint activation. J. Biol. Chem. 2002; 277: 42306–42314

Hunter N, Kleckner N. The single-end invasion: An asymmetric intermediate at the double-strand break to double-Holliday junction transition of meiotic recombination. Cell 2001; 106: 59-70. Doi: 10.1016/S0092-8674 (01) 00430-5

Kaur H, De Muyt A, Lichten M. Top3-Rmi1 DNA single-strand decatenase is integral to the formation and resolution of meiotic recombination intermediates. Mol Cell. 2015;57(4):583–94. doi: 10.1016/j.molcel.2015.01.020 pmid:25699707; PubMed Central PMCID: PMC4338413.

Keeney S, Giroux CN, Kleckner N. Meiosis-specific DNA double-strand breaks are catalyzed by Spo11, a member of a widely conserved protein family. Cell.1997 Feb 7;88(3):375-84. PMID:9039264

Kim KP, Weiner BM, Zhang L, Jordan A, Dekker J, Kleckner N. Sister cohesion and structural axis components mediate homolog bias of meiotic recombination. Cell 2010, 10;143(6):924-37. Doi: 10.1016/j.cell.2010.11.015. PMCID:PMC3033573.

Kohl KP, Sekelsky J. Meiotic and mitotic recombination in meiosis. Genetics. 2013;194(2):327–34. Epub 2013/06/05. doi: 10.1534/genetics.113.150581 pmid:23733849; PubMed Central PMCID: PMC3664844.

Lydall D, Nikolsky Y, Bishop DK, Weinert T. A meiotic recombination checkpoint controlled by mitotic checkpoint genes. Nature. 1996; 383:840–3. pmid:8893012 doi: 10.1038/383840a0

MacQueenAJ, Hochwagen A. Checkpoint mechanisms: the puppet masters of meiotic prophase. Trends Cell Bio. 2011. doi: 10.1016/j.tcb.2011.03.004. PMID: 21531561

Nasmyth K, Peters JM, Uhlmann F. Splitting the chromosome: cutting the ties that bind sister chromatids. Science. 2000; May 26; 288(5470): 1379-85. PMID: 10827941

Niu H, Li X, Job E, Park C, Moazed D, Gygi SP, Hollingsworth NM. Mek1 kinase is regulated to suppress double-strand break repair between sister chromatids during budding yeast meiosis. Mol Cell Biol. 2007;27(15):5456–67. doi: 10.1128/MCB.00416-07 pmid:17526735; PubMed Central PMCID: PMCPMC1952091.

Niu H, Wan L, Baumgartner B, Schaefer D, Loidl J, Hollingsworth NM. Partner choice during meiosis is regulated by Hop1-promoted dimerization of Mek1. Mol Biol Cell. 2005;16:5804–18. PMID:16221890 doi: 10.1091/mbc.e05-05-0465

Niu H, Wan L, Busygina V, Kwon Y, Allen JA, Li X, Kunz RC, Kubota K, Wang B, Sung P, Shokat KM, Gygi SP, Hollingsworth NM. Regulation of meiotic recombination via Mek1-mediated Rad54 phosphorylation. Mol Cell. 2009;36(3):393–404. doi: 10.1016/j.molcel.2009.09.029 pmid:19917248; PubMed Central PMCID: PMCPMC2788773.

Parrilla-Casterllar ER, Arlander SJ, Karnitz L, Dial 9-1-1 for DNA damage: the Rad9-Hus1-Rad1 (9-1-1) clamp complex.2004 PMID: 15279787 doi: 10.1016/j.dnarep.2004.03.032

Petronczki M, Siomos MF, Nasmyth K. *Un menage a quatre*: the molecular biology of chromosome segregation in meiosis. Cell. 2003;112(4):423–40. PMID:12600308. doi: 10.1016/s0092-8674(03)00083-7

Sancar A, Lindsey-Boltz LA, Unsal-Kaxmaz K, Linn S. Molecular mechanisms of mamlian DNA repair and the DNA damage checkpoints. 2004, PMID: 15189136 doi: 10.1146/annurev.biochem.73.011303.073723

Schwacha, A. and Kleckner, N. Identification of double Holliday junctions as intermediates in meiotic recombination. Cell. 1995; 83: 783–791. PMID:8521495

Subramanian VV, Hochwagen A. The meiotic checkpoint network: step-by-step through meiotic prophase. Cold Spring Harbor Perspect Biol. 2014;6(10):a016675. doi: 10.1101/cshperspect.a016675 PMID:25274702

Suhandynata R, Liang J, Albuquerque CP, Zhou H, Hollingsworth NM. A method for sporulating budding yeast cells that allows for unbiased identification of kinase substrates using stable isotope labeling by amino acids in cell culture. G3. 2014;4(11):2125–35. doi: 10.1534/g3.114.013888 pmid:25168012; PubMed Central PMCID: PMCPMC4232538.

Suhandynata R., Wan L., Zhou H., Hollingsworth NM. Identification of putative Mek1 substrates during meiosis in *Saccharomyces cerevisiae* using quantitative phosphoproteomics. PLoS ONE 201611(5): e0155931. doi: 10.1371/journal.pone.0155931

Sung P, Klein H (October 2006). "Mechanism of homologous recombination: mediators and helicases take on regulatory functions". Nature Reviews. Molecular Cell Biology. **7** (10): 739–50. doi; 10.1038/nrm2008. PMID:16926856

Tsubouchi H, Roeder GS. Budd ding yeast Hed1 down-regulates the mitotic recombination machinery when meiotic recombination is impaired. Genes Dev. 2006, July 1; 20(13): 1766-1775. doi: 10.1101/gad.1422506; PMCID: PMC1522073

Wanat JJ, Kim KP, Koszul R, Zanders S, Weiner B, Kleckner N, et al. Csm4, in collaboration with Ndj1, mediates telomere-led chromosome dynamics and recombination during yeast meiosis. PLoS Genet. 2008;4(9):e1000188. doi: 10.1371/journal.pgen.1000188 pmid:18818741; PubMed Central PMCID: PMCPMC2533701.

Wan L., de los Santos T., Zhang C., Shokat K., Hollingsworth NM. Mek1 kinase activity functions downstream of *RED1* in the regulation of meiotic double strand break repair in budding yeast. Mol Biol Cell. 2004;15(1):11–23. doi: 10.1091/mbc.E03-07-0499 pmid:14595109; PubMed Central PMCID: PMCPMC307523.

Wu HY, Burgess SM. Two distinct surveillance mechanisms monitor meiotic chromosome metabolism in budding yeast. Curr Biol. 2006;16(24):2473–9. doi: 10.1016/j.cub.2006.10.069 pmid:17174924; PubMed Central PMCID: PMCPMC1876825